FLEXIBLE AND TRANSPARENT MICROCAVITY PLASMA DEVICES: FABRICATED BY POLYMER-BASED REPLICA MOLDING TECHNIQUE

BY

SUNGKUN LEE

THESIS

Submitted in partial fulfillment of the requirements
for the degree of Master of Science in Materials Science and Engineering
in the Graduate College of the
University of Illinois at Urbana-Champaign, 2010

Urbana, Illinois

Adviser:

Professor J. Gary Eden

ABSTRACT

The fabrication of flexible and transparent microplasma devices using plastic substrate has explored new avenues in plasma science and technology. A polymer-based replica molding process enables inexpensive and accurate production of microcavities of the devices. Best known as the sources of visible, ultraviolet (UV) and vacuum ultraviolet (VUV) radiation, microplasma devices fabricated by replica molding techniques also show potential applications as transparent and flexible displays, a radiation source for medical phototherapy, and photonic circuit light sources. In this thesis, the basic physics of plasma discharges is discussed and the performance and fabrication of microplasma devices by a replica molding process is presented in detail.

To Father and Mother

ACKNOWLEDGMENTS

First of all, I would like to thank God for all the blessings he brings into my life and hub of enlightening wisdom he allows me to make my research possible. This project at the Laboratory for Optical Physics and Engineering would not have been possible without the support of my parents and other fabulous people around me. Many thanks to my advisers, Professor J. Gary Eden and Professor Sung-jin Park who offered guidance and faith to encourage me to gain a wealth of knowledge and overcome challenges during the project. Thanks to my colleagues for Seung Hoon Sung, Taek Lim Kim, and Jekwon Yoon for their great support and assistance for my research.

TABLE OF CONTENTS

CHAPTER 1

INTRODUCTION

Microplasma is a new subclass of plasma defined as a weakly ionized, low temperature, nonequilibrium plasma having characteristic dimensions ranging from 1 mm to 1 μm [1]. Spatially confining plasma to microcavities has opened a new approach to generating and maintaining stable glow discharges at atmospheric pressure [2]. Microplasma is also known for extremely high power loadings of 10^4 to 10^6 W/cm^3, and electron densities up to 10^{16}/cm^3, which are difficult to achieve with macroplasma. These attractive behaviors of microplasma open a new and fascinating realm of plasma science and its applications which require efficient sources of ultraviolet (UV), visible, or vacuum-ultraviolet (VUV) radiation, such as in medical diagnostics, displays, and environmental sensing [2].

Microplasma devices have been studied for more than four decades and designed for operation as the source of incoherent vacuum ultraviolet (VUV) radiation for plasma display panels [3], [4]. Several different microplasma devices have been investigated at the Laboratory for Optical Physics and Engineering (LOPE) at the University of Illinois. These microplasma devices have been fabricated by different techniques on various substrates which include aluminum, glass, and plastic substrates. The purpose of each device is unique based on applications, but they all stem from the same basic concept of microcavity plasma.

In particular, microplasma devices in fabricated with a plastic substrate have been of interest since flexible and transparent photonic/electronic products are expected to take a major share of the future electronics market. The polymer-based replica molding process by which flexible transparent microplasma devices are fabricated enables the accurate and inexpensive production of microcavities [5].

Although many microcavity plasma devices are flexible [6]-[8], a flexible design that is also transparent has not yet been developed. The research discussed in this thesis focuses on the development of novel microplasma devices and arrays by a replica molding technique in which the substrate is a flexible and transparent plastic film [4]. In addition to the fabrication process for these plastic-based microplasma devices, research has been performed to access promising applications such as flexible displays, medial phototherapy, and ultraviolet light sources.

CHAPTER 2

BACKGROUND

2.1 Plasma Physics in DC discharge

Plasma physics describes the movements and interactions between electrons, ions, and gas atoms or molecule. When a potential difference such as a DC voltage, is applied between two electrodes in a gas, positive ions accumulate near the negatively biased cathode and electrons are repelled from the cathode, which creates a positive space charge. This space charge is responsible for forming a sheath region in which the electron density is much lower than the ion density.

The luminous glow of a plasma is produced by electron impact of collisions. In order to maintain the steady state, there should be a continuous and an equal degree of ionization. One of the most important electron generation mechanisms in a plasma is that of secondary electron emission in which ions are accelerated towards the cathode. These electrons are accelerated by the high electric field in the sheath and may lose energy through elastic and inelastic collisions with neutrals and ions. Acquiring sufficient energy from the electric field permits the collision of electrons with neutrals in the sheath and glow regions to electronically excite and ionize atoms and molecules, processes which often culminate in emission. One strong region of emission is the negative glow region, the brightest intensity of the entire discharge. Electrons carry most of the current virtually everywhere.

For ions to enter the sheath region as they move toward the cathode, the velocities of ions satisfy the Bohm sheath criterion:

$$u_s \geq u_b = \left(\frac{eT_e}{M}\right)^{\frac{1}{2}}$$

where u_s is ion velocity at sheath, u_B is the Bohm velocity, T_e is electron temperature, and M is the mass of the ion.

The region between bulk plasma and the sheath is known as the presheath in which the electron and ion densities are the same. Figure 2.1 shows the structure of the cathode sheath in a DC driven plasma.

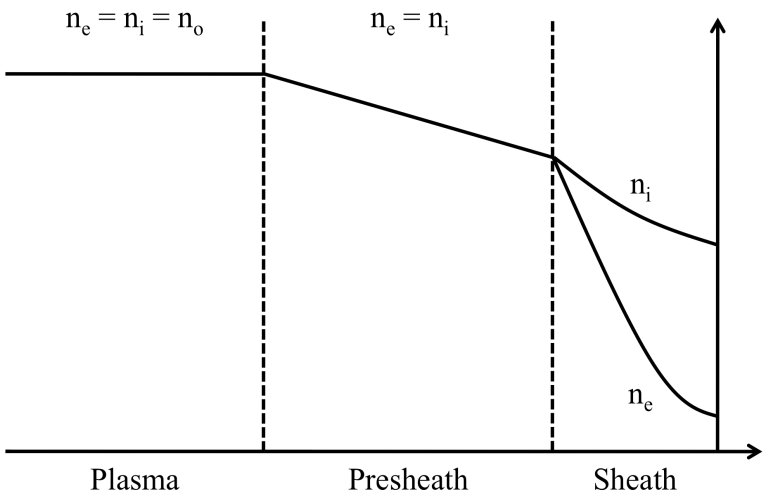

Figure 2.1 The structure of the non-neutral sheath and presheath regions of the plasma in the region adjacent to the cathode region.

The non-neutral sheath and presheath regions of the plasma adjacent to the cathode are even more important since classical discharge theory ventures into new territory when the characteristic dimension of the cavities is scaled down to micrometers and eventually shrink to the same order of magnitude as the plasma Debye length.

In this case, the thickness of the sheath region at the cathode occupies a large portion of the entire cavity, and is the dominant factor in determining the behavior of the plasma. The positive column shrinks first and eventually is unable to form as the plasma cavity size decreases further.

2.2 Microcavity Plasma

Microcavity plasmas are defined as weakly ionized, low temperature, non-equilibrium plasmas spatially confined to cavities with a characteristic dimension of a few micrometers up to a few hundreds of micrometers [1]. Microplasma cavities with power loadings of 10^4 to 10^6 W/cm^3 and electron densities up to 10^{16} cm^{-3} have exhibited their stable operation at pressures greater than one atmosphere. This result can be expected from Paschen's law [18], which states that the breakdown voltage of a gap is a function of the product of the gas pressure and the length of the gap:

$$V_B = f(pd)$$

where V_B is the breakdown voltage, p is pressure, and d is the gap distance.

Illustrated in Fig. 2.2, Paschen's law says that the same breakdown voltage can be obtained at higher pressures by reducing the gap distance [9]. This fact provides high motivation for the development of microcavity plasma devices which can operate at atmosphere pressure or beyond.

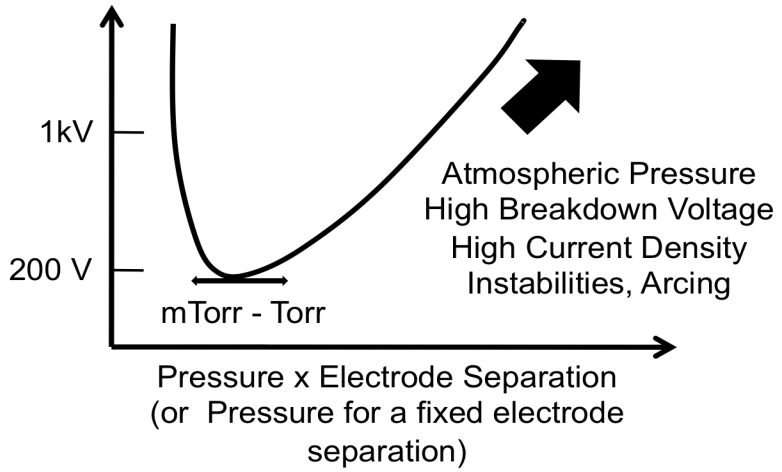

Figure 2.2 Schematic diagram of Paschen's curve, which illustrates the variation of the discharge breakdown voltage with the (*pd)* product [9].

For the microplasma devices represented by the portion of the curve that has negative slope, $pd \cdot (\lambda_{sheath}/d)$ scaling has been introduced where λ_{sheath} is the thickness of sheath [2]. As the dimensions of the microcavities become smaller and the ratio of the surface area to volume rises, microplasma behavior is increasingly dominated by wall interactions. As the ratio of surface area to volume increases, the process of secondary electron emission, which plays a critical role in sustaining a glow discharge, generates more electrons because of more interactions between electrons and the wall.

For the microplasma devices, the turn-on voltage of the device is proportional to the breakdown voltage. Gas pressure *p* can be controlled externally, and therefore, the only factor to be considered for the fabrication of the device is the distance between the electrodes, which would be the same as the thickness of the dielectric material deposited on the two substrates.

The recent realization of microplasma devices fabricated on plastic substrates by replica molding processes which are easy and a low-cost fabrication method has offered new era of microplasma science. The replica-molding techniques offers the capability for reproducibly fabricating features with dimensions under a few micrometers and high aspect ratios (channel length: width greater than 10^3:1) [4]. The fabrication of flexible, optically transparent and lightweight arrays of microplasma devices by replica-molding suggests a unique class of microplasma technology [19]. Future applications of microplasma devices fabricated by replica-molding include transparent and flexible displays, ultra-violet light source for on-chip biomedical phototherapy, and photonic devices [10].

CHAPTER 3

EXPERIMENTAL METHODS

3.1 Design of Flexible Microplasma Device on Plastic Substrate

Several different microplasma devices have been designed and fabricated in order to better understand the electrical and optical properties of the devices built onto plastic substrates.

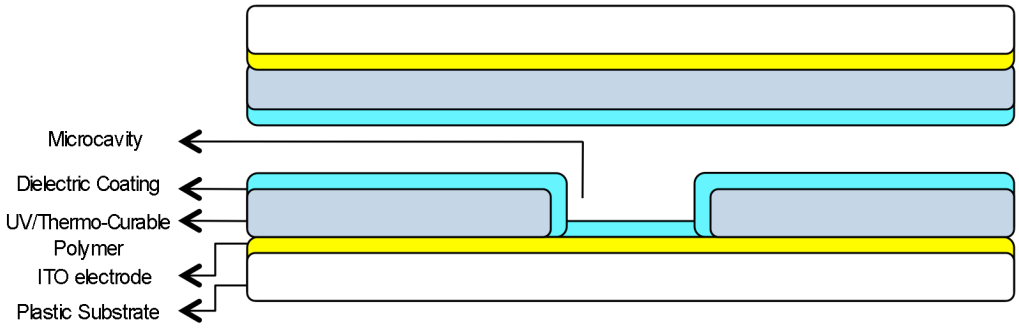

Figure 3.1 Generalized diagram of a typical microplasma device fabricated by replica molding technique in plastic substrate.

Fig. 3.1 shows the typical structure of a replica-molded microplasma devices. It is formed by bonding two substrates having different patterns. The substrate is of a micron of a flexible polyethylene terephthalate (PET) film having a less than 0.5 μm coated with a conducting ITO layer, which has the thickness of 0.12 μm. The ITO film constitutes the bottom electrode of the microplasma device. The microcavities are defined within a layer of UV-curable polymer or thermo-curable polymer which has been imprinted with the desired cavity and channel pattern by the replica-molding process [5], [11]. Following the replication of microplasma cavity in a transparent polymer material, a thin film dielectric material, which includes silicon dioxide, titanium dioxide, magnesium oxide, or silicon nitride is deposited to protect microcavities on the polymer layer from exposure to plasma. Ions in the sheath region of plasma are accelerated toward the cathode and gain energies of hundreds of eV before colliding

with the surface, which can cause degradation of plasma devices based on a plastic substrate. The dielectric layer also reduces the rate of outgassing as it seems as a barrier to organic vapors evaporating from the polymer [4]. For the most efficient operation of the device, the control of this dielectric protective coating is important since it affects the overall capacitance of the device. The upper electrode in Fig. 3.1 is an ITO-coated PET film, which is bonded to the top of the polymer microcavities. After the cover is bonded to the lower portion of the structure, electrical leads are attached to both the upper and lower electrodes, and gas is introduced to the interior of the device, through an opening made in one of the substrates.

3.2 Fabrication of Microplasma Device by Replica Molding Technique

The fabrication of microcavity plasma devices on plastic substrates begins with preparing a silicon "master" wafer with a positive volume image of the microcavities for UV-curable polymer, and a negative volume image for thermo-curable polymer. After basic degreasing steps and native oxide removal, the positive photoresist, AZ4620 is dispensed onto a 4-in-diameter (100 mm) wafer. Exposed with the patterned mask and developed, the wafer is treated with a descum process to remove completely the photoresist residues in the developed area of the pattern. Then, cavity patterns are etched by inductively coupled plasma (ICP) reactive ion etching (RIE) with the Bosch process in a pulsed or time-multiplexed etching sequence which provides a cavity depth of 70 μm.

In order to transfer the pattern of the microcavities onto the silicon wafer by soft lithography, a polydimethlysiloxane (PDMS, DuPont Sylgard 184) silicon elastomer mold was made. It is poured onto the repellent-treated wafer and is cured at 100°C for a few hours to exhibit a mechanically flexible characteristic. Separation between the PDMS stamp and the master wafer is enhanced by pretreatment of the wafer with Repel Silane (GE Healthcare), which

offers an antiadhesion monolayer coating. The microcavity pattern is produced by a liquid UV-curable polymer introduced between the PDMS and the plastic substrate. The liquid polymer flows into the mold shape and is cured by high intensity UV light. After UV illumination, the PDMS mold is released from the replica of the microcavity pattern. Since the cured polymer adheres to the plastic substrate, the PDMS mold can be used repeatedly. Following the replica molding process, a dielectric barrier film, SiO_2 or TiO_2, with a thickness of 300 nm is deposited by the e-beam evaporator system to protect the microcavity from exposure to the plasma as well as to prevent outgassing from the polymer layer. To bond the cover with the bottom substrate, UV-curable polymer is dispensed on the polymer patterned substrate and spun to provide a thick and uniform layer of adhesive. Then, the cover substrate is slowly placed on the replicated pattern of the bottom layer and cured by UV illumination for 80 seconds. Fig. 3.2 below summarizes the basic fabrication steps of the replica molded microplasma devices.

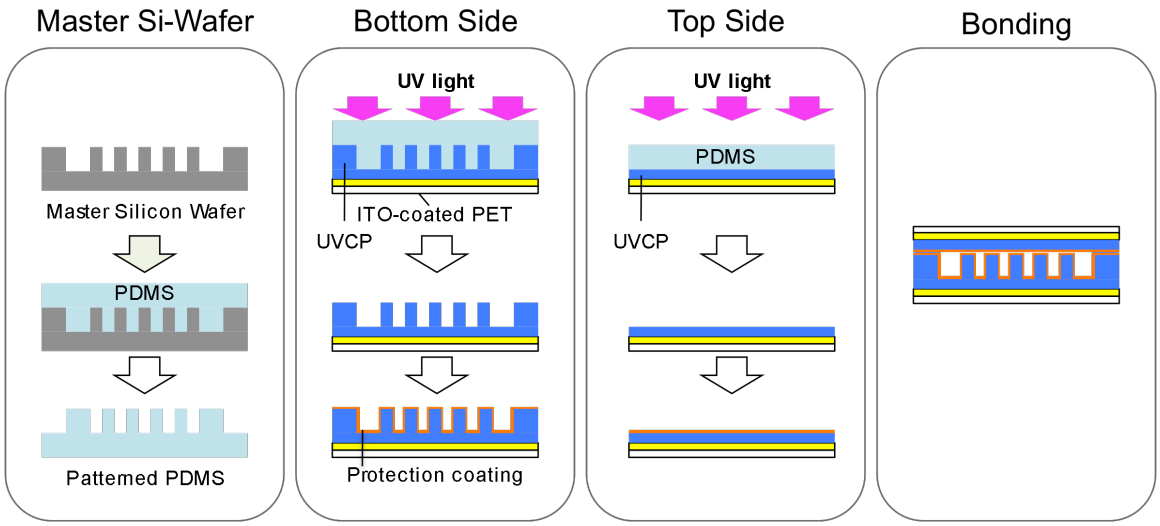

Figure 3.2 Schematic diagram of fabrication steps of replica molding devices.

Ultraviolet-curable polymer (Type SK-9, Optical Cement) has been used as the dielectric material for the device because of its excellent UV curability at 365 nm and transparency as well as good adhesion to plastic substrate. In addition, the polymer which has a viscosity of

approximately 80 cps enables the replication of pattern by soft lithography without forming air bubbles. Recently, further investigation has found that a silicone (RTV, GE) is a better dielectric material and dramatically improves the mechanical flexibility of the device while maintaining the properties of optical transparency and excellent adhesion to plastic. Unlike UV-curable polymer, silicone maintains outstanding mechanical flexibility after it is cured. For fabrication using silicone as the dielectric layer, a PDMS mold is not necessary, a which reduces cost and processing time. Therefore, the silicon master wafer contains a negative image of the desired microcavity pattern and is used directly to replicate the pattern on the plastic substrate.

3.3 Vacuum System and Testing Environment

Before loading and testing the microplasma devices, having a high quality vacuum system is required. The schematic diagram in Fig. 3.3 shows the testing environment of the replica-molding microplasma device. The vacuum system is composed of a main chamber, a gas inlet connected to a gas cylinder, a roughing pump, a turbomolecular pump, and two types of pressure gauges: a capacitance manometer and an ionization gauge. The roughing pump evacuates the main chamber down to pressure of a few millitorr and the turbomolecular pump, to pressure of 10^{-8} Torr. After five to six hours with the turbomolecular pump on, the testing environment is evacuated to a base pressure of less than 10^{-6} and is subsequently backfilled with the desired gas mixture for device testing. For the measurement of the device operating pressure, two capacitance manometers and an ionization gauge are used. Microplasma devices are connected to a high voltage AC power supply, providing RMS voltages at a driving frequency of 20 kHz.

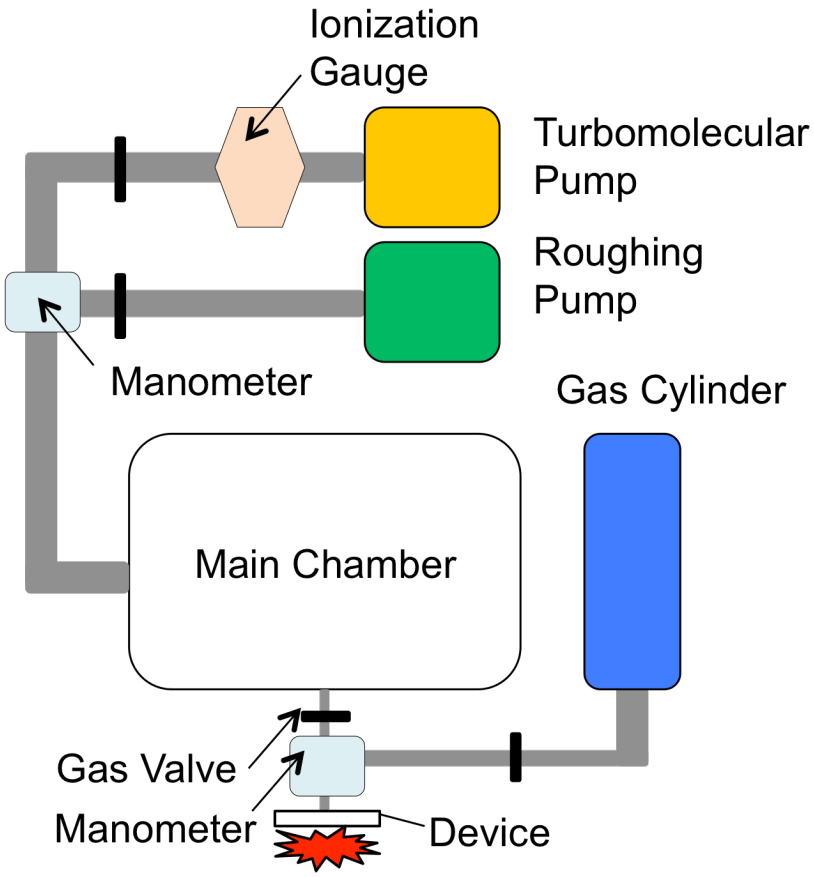

Figure 3.3 Schematic diagram of the vacuum system

CHAPTER 4

RESULTS AND DISCUSSION

4.1 UV Emission from Microplasma Devices on Plastic Substrates

It is known from previous studies in the Laboratory for Optical Physics and Engineering that neon gas is a good choice for testing microplasma devices since operating voltage usually is lower than those for other gases mixtures such as Ar, and the emission lies predominately visible. Operation of the an array of microplasma devices on a plastic substrate by the replica molding process is shown in Fig. 4.1 for Ne at a pressure of 500 Torr.

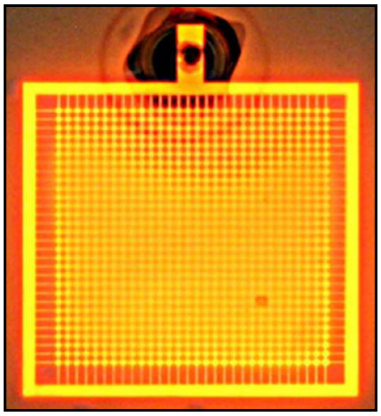

Figure 4.1 Operation of a 30×30 array of 200-μm diameter cavities in Ne at 500 Torr.

The operation of the replica molded devices in plastic in Fig. 4.1 suggests that there is a promising approach to fabricating microplasma devices in an inexpensive, flexible, and transparent substrate that is also disposable and recyclable. The ultimate goal of a replica molding device is to create a flexible and transparent display panel which emits visible colors, and to realize an on-chip biomedical device for phototherapy. Both applications require microplasma devices to emit a significant amount of UV light. A mixture of 97% argon and 3% of nitrogen has been tested and the emission spectrum of Fig. 4.2 demonstrates that the expected

UV emission at 337.1 mm [12], 357.7 nm, 380.5 nm, and 405.9 nm [13] is, indeed, generated. Therefore, even though the device is turned on in neon gas with lower voltage, an argon-nitrogen mixture is chosen to serve as the operating plasma for the replica-molded devices. Figure 4.3 is a photograph of a 5×5 show that the device illuminated in front of a one dollar bill to show the device is fully transparent.

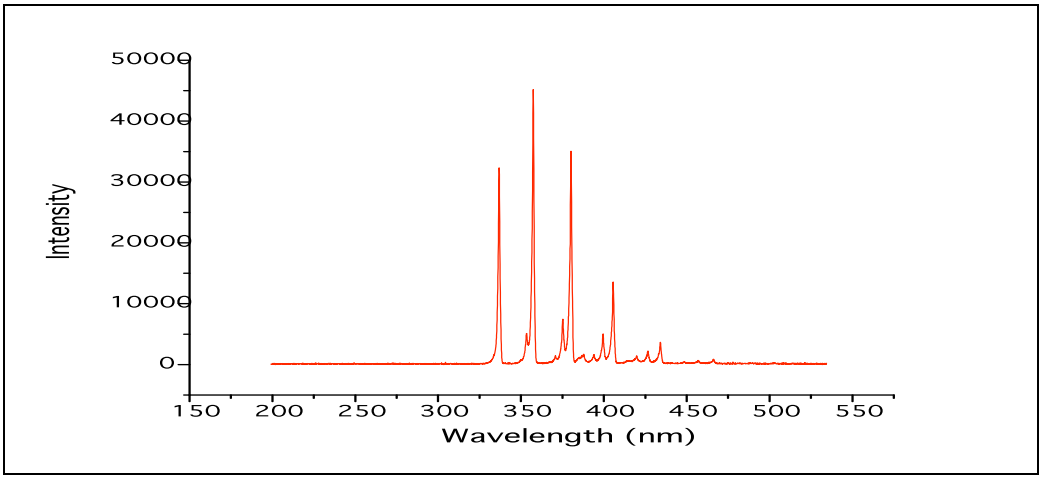

Figure 4.2 Emission spectra from device operation in Ar-N_2 gas mixture

Figure 4.3 Photographs of 5×5 array of cavities in front of dollar bill. Operation of device in Ar-N_2 mixture at 250 Torr.

The turn-on voltage of the device having the Ar-N_2 mixture, 1.2 $kV_{peak-peak}$ is higher than that 760 V of the device in neon from Fig. 4.1. Despite the higher voltage required, both the display device and biomedical device make use of an Ar-N_2 mixture. Therefore, one important

observation is that the device survives in operation with the mixture and shows its potential as a UV emitting source.

4.2 Flexible and Transparent Device I: RGB Generation by Dye or Phosphor Excitation

One of the goals in this research is to fabricate a transparent and flexible display unit using dyes embedded in microcavities of the device. Since experiments show that the device operates in an Ar-N_2 mixture producing UV emission [12], several organic dyes are chosen to generate visible colors excited by UV emission of the device. Dyes chosen for the devices are Rhodamine 640 (Exciton), Rhodamine 590 (Exciton), and Coumarin 460 (Exciton) to generate red, green, and blue respectively. Extensive research was performed to determine the appropriate solvent for the dye such that the dye solution mixed with UV-curable polymer can be excited by UV light while maintaining its transparency. In Fig. 4.4, ethylene glycol is successful in dissolving dyes and maintains its transparency. Able of being mixed to a single phase with UV-curable polymer and yet not dissolving the polymer, ethylene glycol is chosen as the solvent for the dye and UV-curable polymer.

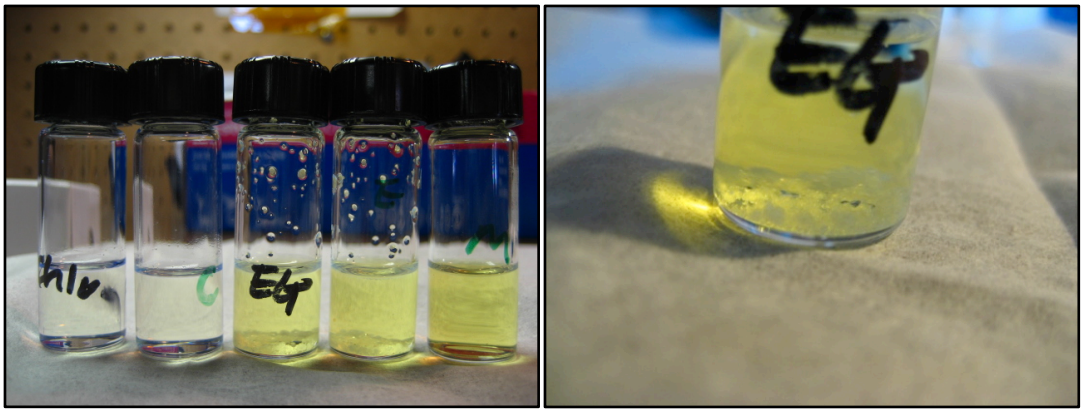

Figure 4.4 Solubility test to choose the solvent for dye and UV-curable polymer

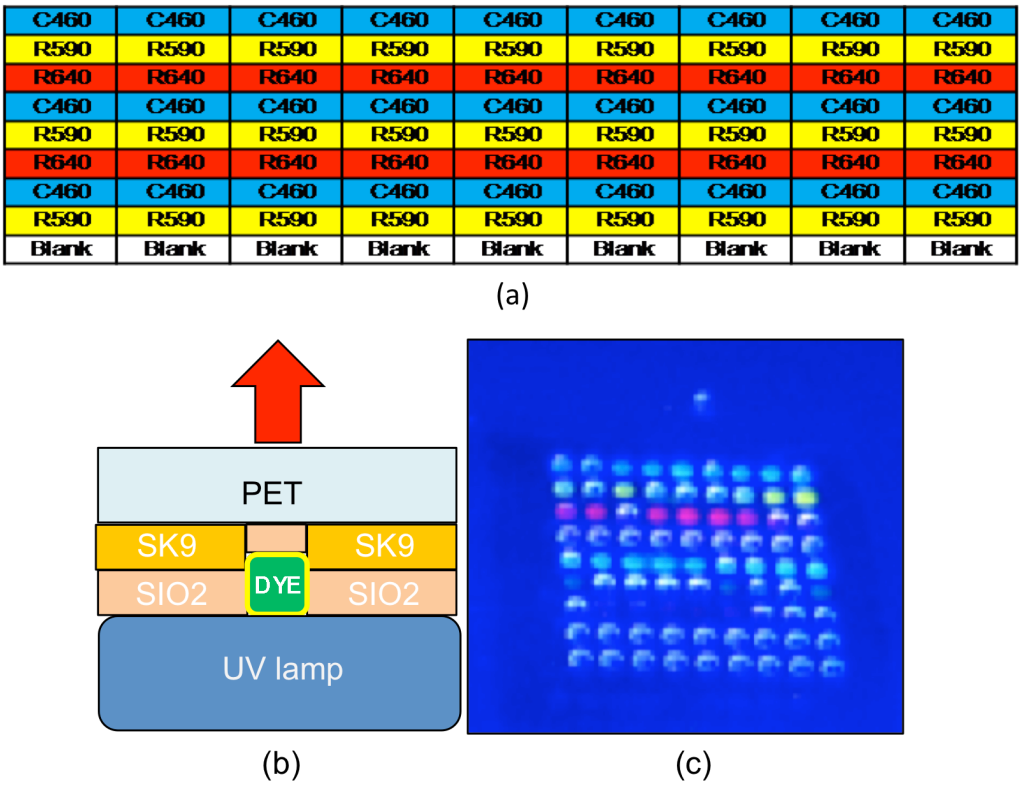

Figure 4.5 (a) Arrangement of dyes in microcavities. (b) Schematic diagram that shows dyes on patterned plastic substrate with UV lamp. (c) Excitation of dyes by UV lamp in (b).

In panel (a) of Fig. 4.5, the pattern of dyes incorporated into microcavities is shown. Fig. 4.5 (b) is a cross-sectional diagram of the structure of a single pixel designed to emit a particular color and spectrum. Part (c) of Fig. 4.5 is a photograph of a 9×9 array of pixels, each having a specific dye, illuminated by an UV lamp. Fig. 4.6 shows that dyes are still excited by UV lamp to generate visible colors after installing the cover plastic substrate.

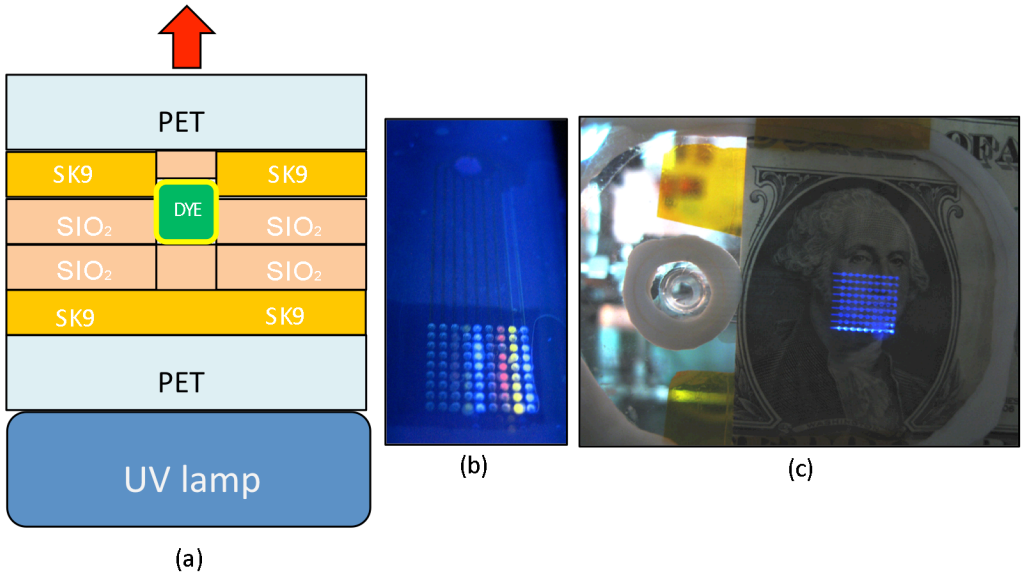

Figure 4.6 (a) Schematic diagram of complete device with dyes embedded. (b) Excitation of dyes under UV lamp. (c) Operation of device in Ar-N_2 mixture

As shown in Fig. 4.7, however, under operation of the device, the visible colors arising from excitation of the dyes are not observed. Since the hydroxyl radicals produced by the plasma are known as to be a strong oxidizing agent which might bleach the solution and degrade the solute [14], we concluded that the dye is degraded by the plasma during plasma operation. Therefore, in next device fabrication, a 300 nm thick, additional layer of SiO_2 is deposited to protect the dyes from being oxidized. Fig. 4.8 shows the operation of the device under Ar-N_2 mixture and colors of red, yellow, and blue are clearly obtained.

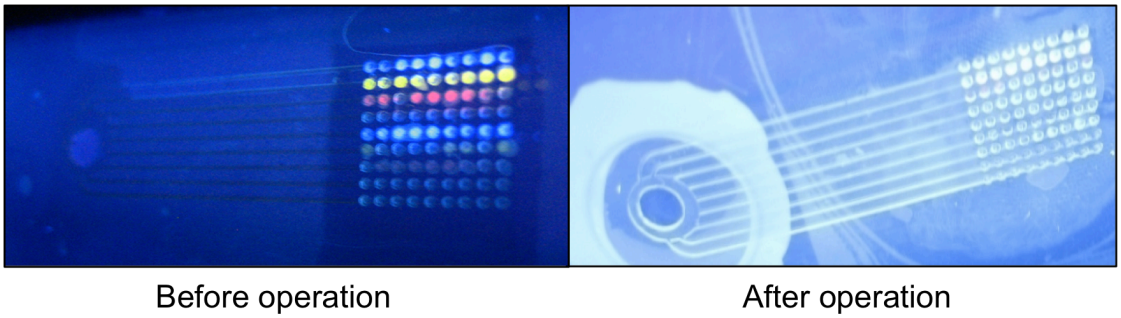

Figure 4.7 The devices under UV lamp before and after operation

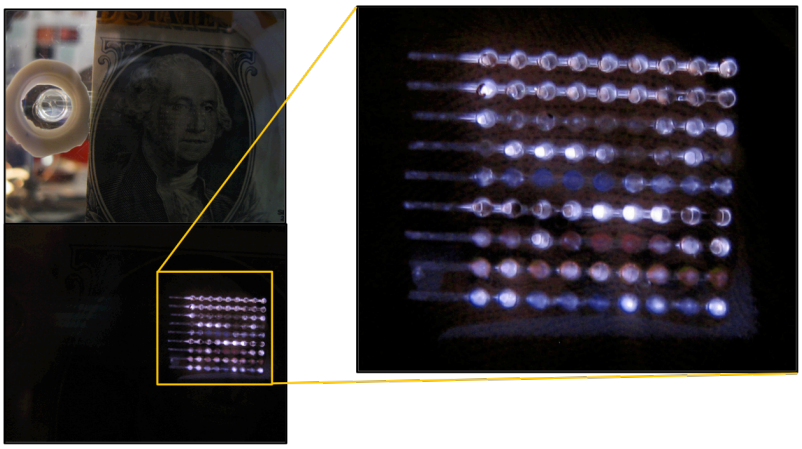

Figure 4.8 The operation of device with additional protective layer of SiO_2

While transparent replica molded devices are now improved to generate visible colors from chemical dyes, studies were performed to find an alternate dielectric material offering devices with better flexibility than UV-curable polymer as to fabricate a “fully flexible” and transparent display unit. Silicone-based polymer was introduced to replace the UV-curable polymer since silicone rubber such as RTV615 (GE) possesses a high degree of flexibility at lower temperatures and yet is stable to temperatures as high as 204°C, while maintaining excellent electrical properties as well as good biocompatibility. The fabrication procedure for the device with silicone rubber as the dielectric material is the same as that for the UV-curable polymer except the PDMS mold is not necessary and the pattern is directly replicated from the master silicon wafer to the plastic substrate. Therefore, the master silicon wafer will have the negative image of the desired pattern of the device. Before fabricating devices with silicone rubber and chemical dyes, Fig. 4.9 shows several experiments to observe the solubility of a particular dye with a solvent, excitation after mixing the dye with silicone, and after thermal cure. It is clear in Fig 4.9 that Rhodamine 640, Disodium Fluorescein, and Rhodamine 590 are degraded after thermal treatment, which is necessary for curing the silicone polymer. Therefore,

instead of chemical dyes, phosphor was chosen as the wavelength conversion medium because of its stability at higher temperatures.

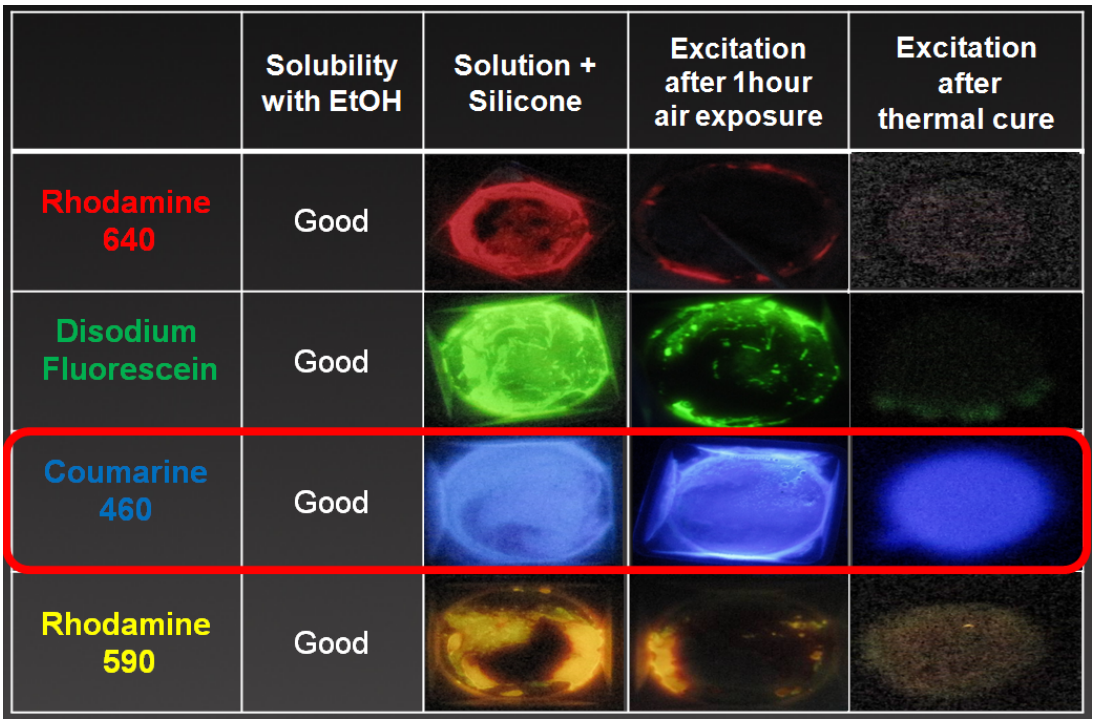

Figure 4.9 Solubility with solvents and excitation of dye by UV lamp before and after thermal cure

The same test for excitation of the silicone and phosphor after thermal cure is shown in Fig. 4.10. It clearly demonstrates that the phosphor emits vivid RGB colors instead of being degraded after thermal cure.

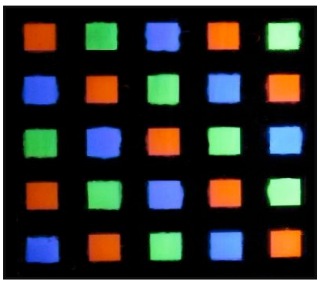

Figure 4.10 Excitation of phosphor mixed and cured with silicone rubber and placed under a UV lamp.

However, during the first few trials of test, the device with phosphor embedded inside microcavities were not ignited by the plasma discharge. Continued observations of failures of the device suggested that one possible reason is that phosphor is blocking of gas cavity by phosphor excess. As a precaution to prevent phosphor from blocking the gas cavities, Fig. 4.11 illustrates the addition of another protection layer of silicone rubber on top of the phosphor-contained silicone layer.

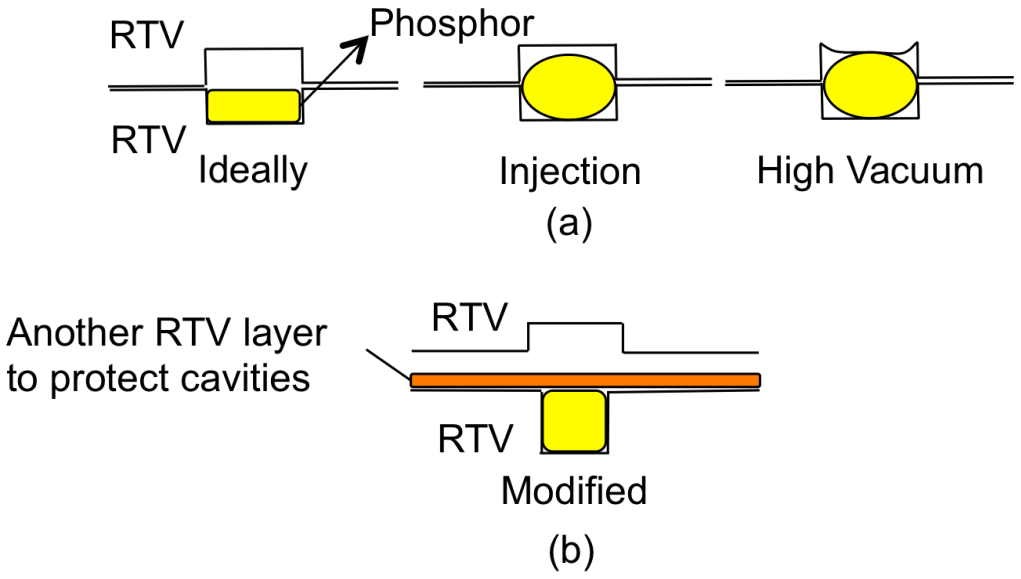

Figure 4.11 (a) Possible way for phosphor to block the gas cavity, preventing a discharge within the cavity; (b) Another silicone layer dispensed and cured on the top of the silicone layer which contains phosphor to prevent phosphor blocking of the gas cavity.

Fig. 4.12 demonstrates the excitation of the phosphor embedded in a small array of the plastic substrate by a UV lamp, showing its excellent flexibility at the same time.

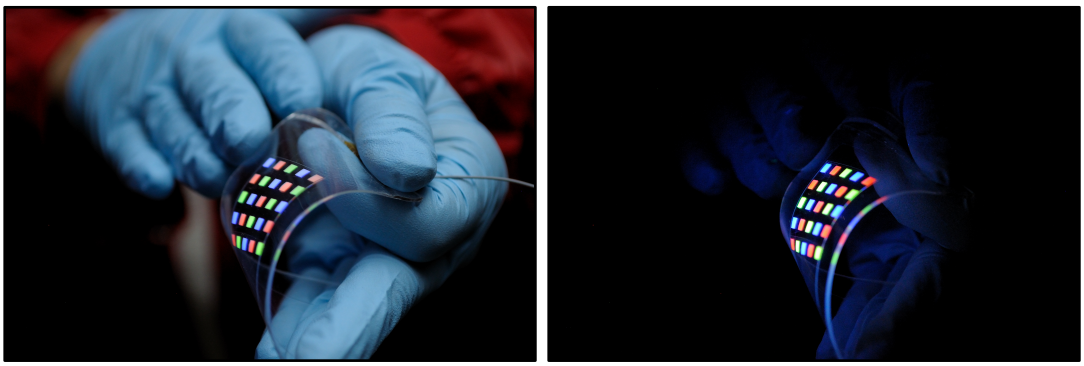

Figure 4.12 Excitation of phosphor embedded in a small array of the plastic substrate, exhibiting the flexibility of the substrate.

Fig. 4.13 illustrates the operation of a small array of device fabricated with the improvement of Fig. 4.11 (b). Finally, by generating RGB colors through the excitement of phosphors by Ar-N_2 emission from a plasma discharge, a fully transparent and flexible microcavity plasma device has been achieved.

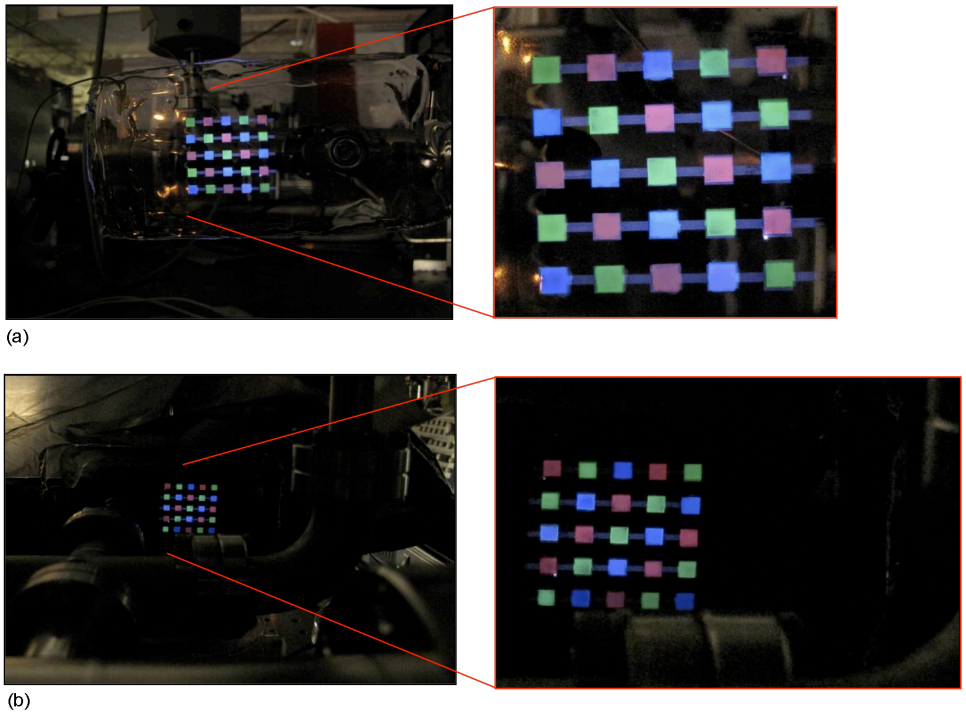

Figure 4.13 Operation of a final device in an Ar-N_2 mixture, successfully generating three RGB colors. (a) Front and (b) back views under operation.

4.3 Flexible and Transparent Device II: Biomedical Application

While plastic-based microplasma devices that generate RGB colors have been successfully fabricated, thus demonstrating the application of this technology to displays, another motivation was to utilize these replica molded devices for biomedical phototherapy applications. Previous research reported by our laboratory demonstrated that with Ar-D_2 (Deuterium) mixture, the operation of silicon microplasma devices shows a broad band of emission spectrum ranging from 250 nm to 450 nm with peak emission at 310 to 315 nm [15]. The spectrum reported in reference 15 is shown in Fig 4.14.

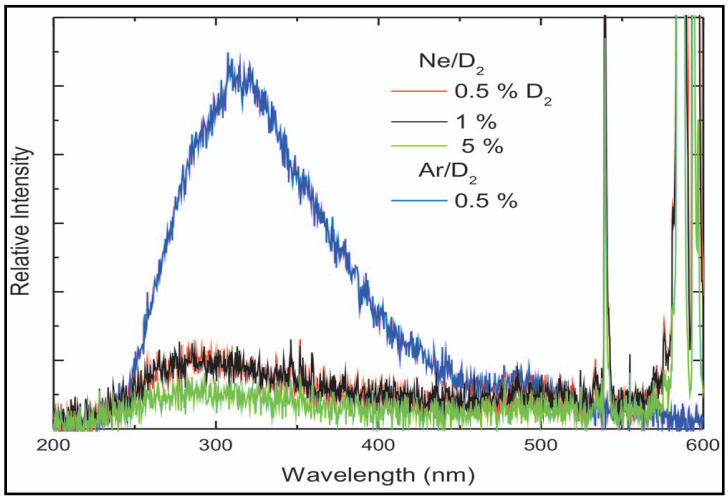

Figure 4.14 Emission spectra in the 200-600 nm wavelength region, produced by Ne/ (0.5%-5%) D_2 and Ar/0.5% D_2 gas mixtures in 50 × 50 arrays of Si microcavity plasma devices [15].

It is known that UV light at sufficiently short wavelength can be used to break down microorganisms, a process which has applications as food preservation, and air and water purification. Currently, most of medical devices which serve germicidal function are heavy, complex, and expensive. Therefore, one goal of this research is to utilize the replica-molding process and fabricate inexpensive, flexible, and light-weight microplasma devices to serve as a

UV emitting bandage which emits wavelength ranging from 250 nm to 380 nm for biomedical applications.

The device fabrication steps are basically the same as those for the previous replica-molded microplasma devices. The 25 × 25 array of microchannels is chosen as the pattern to maximize the amount of UV emission from the device. A device fabricated by replica molding technique is shown in Fig. 4.15, showing complete transparency as well as the flexibility of the device. Fig. 4.16 presents two photos of the plasma device shown in Fig. 4.15 operating in 300 Torr of neon (a) or an Ar-D_2 mixture (b).

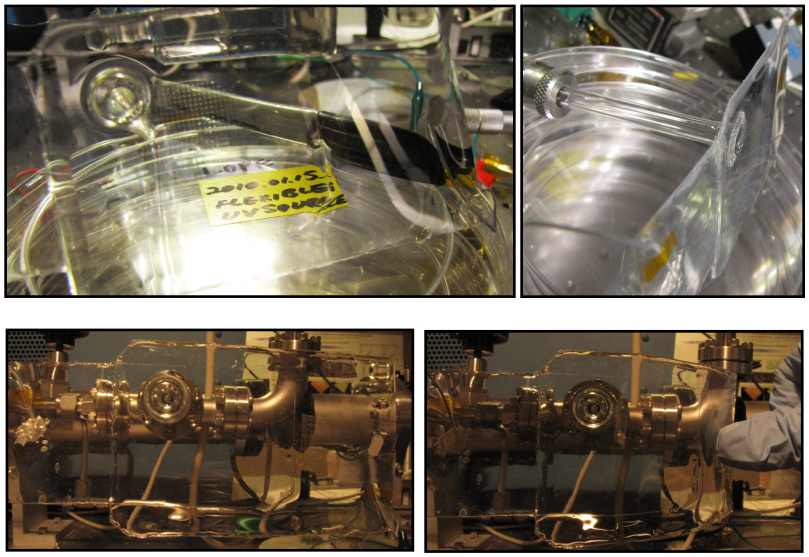

Figure 4.15 Thin, flexible and transparent microplasma device for UV emitting source. Top two photographs show the front and side views of the device. And bottom two, the device loaded before testing.

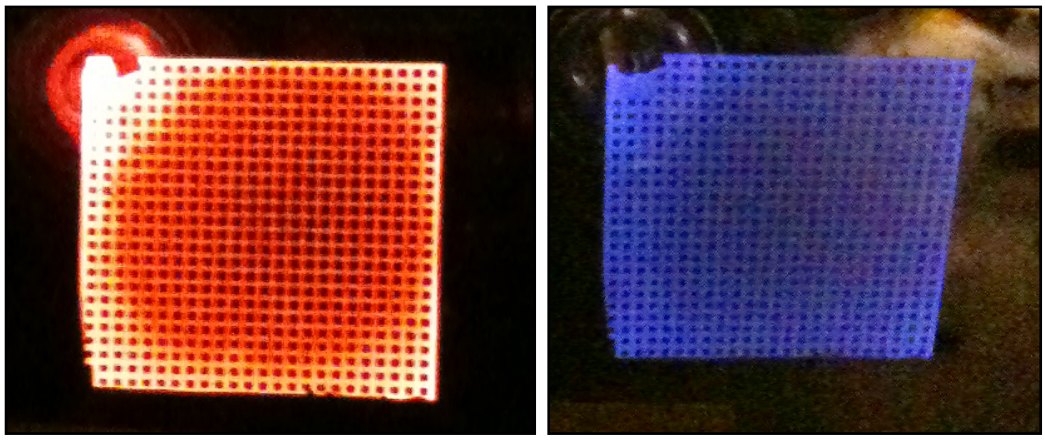

(a) (b)

Figure 4.16 The 25 × 25 array microchannel devices operating at 300 Torr of Ne (a) and Ar-D_2 mixture (b).

Emission spectra in the 200 nm to 600 nm region are shown in Fig. 4.17. Even though it is expected that the spectrum has a broad band of emission in the 250 nm to 450 nm region, the emission does not extend below ~300 nm.

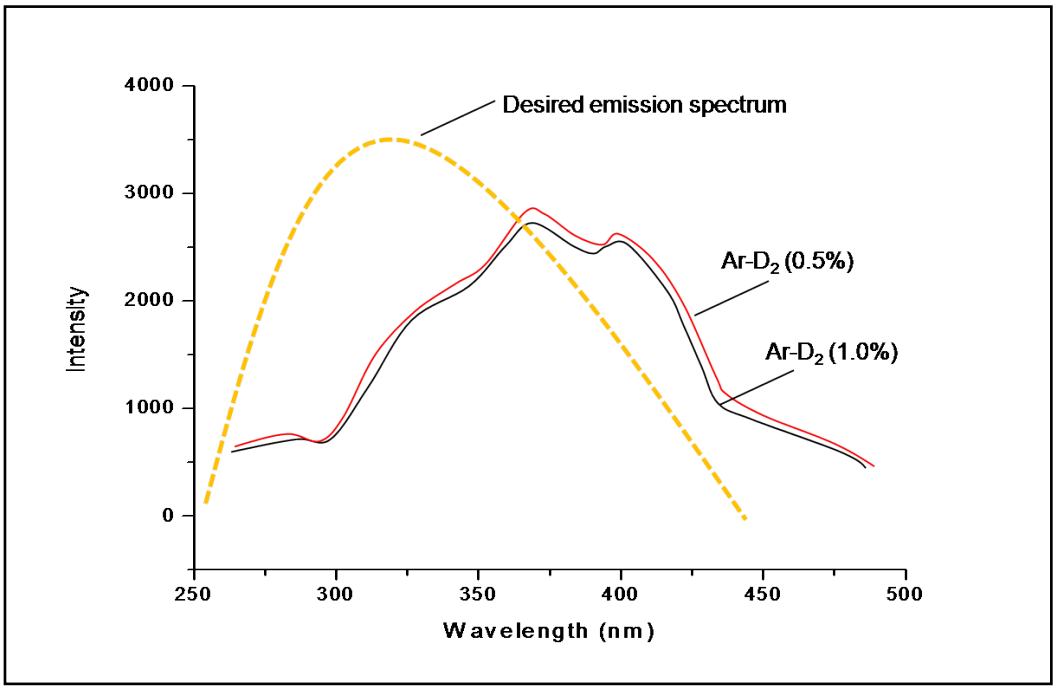

Figure 4.17 Emission Spectra in 250 nm to 600 nm wavelength region produced by Ar-D_2 mixture with 0.5% D_2 (a), 1.0% D_2, and desired emission spectrum (c).

From several studies on materials used for the devices, it is found that PET with an ITO coating is responsible for the cut-off of short UV wavelength in the emission spectrum shown in Fig. 4.18 [16], [17].

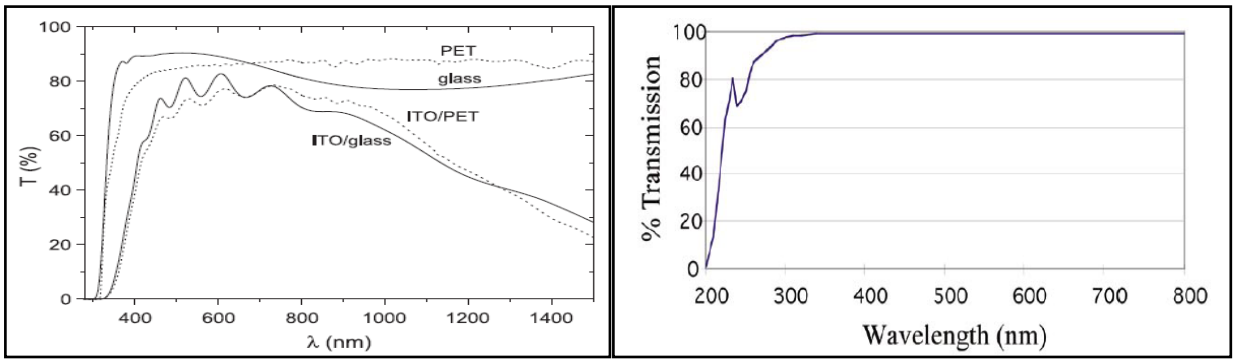

(a) (b)

Figure 4.18 Optical transmittance spectra for (a) PET, glass, ITO/PET, and ITO/glass [16], and (b) 1 mm thick PDMS elastomer [17].

As illustrated in Fig. 4.18, PDMS has excellent transmission from 200 nm to 300 nm in which PET with an ITO coating has low transmission. Therefore, in order to improve the performance of the devices with regard to short wavelength emission, future fabrication should replace the PET/ITO cover of the device with PDMS and an electrode pattern.

4.4 Conclusions

Microplasma devices fabricated on plastic substrate have been operated successfully and tested in various gases such as Ne, Ar, or the Ar-D_2 mixture. Both a novel fabrication process of replica molding and extensive research on materials have led to the realization of transparent and flexible microplasma devices. As one of the goals for this research, the generations if color by chemical dyes as well as phosphors has been achieved, thus demonstrating a promising approach realizing flexible and transparent displays. The next step for the display device is to shrink the

size of the cavities and to pattern sophisticated electrode structures for addressability. More studies on chemical and organic dyes should be continued to improve color generation. In addition to the display device, microplasma devices fabricated by plastic-based replica molding have been optimized for biomedical applications. Numerous experiments have been done to fabricate a flexible, inexpensive, and thin device which emits short wavelength UV light. To yield stronger emission of $\lambda <$ 300 nm UV radiation, PET/ITO as the top cover should be replaced with a PDMS layer on which electrodes are patterned since a PDMS shows excellent optical transmittance in the 200 nm to 300 nm range. Lastly, for both display and biomedical devices, optimization of the device structure so as to decrease the operating voltage should be performed.

REFERENCES

[1] S. J. Park, J. Chen, C. J. Wagner, N. P. Ostrum, C. Liu, and J. G. Eden, "Microdischarge arrays: A new family of photonic devices," *IEEE J. Selec. Topics Quantum Electronics,* vol. 8, p. 387, 2002

[2] K. H. Becker, K. H. Schoenbach, and J. G. Eden, "Microplasmas and applications," *J. Appl. Phys. D,* vol. 39, no. 11, p. R55, 2006

[3] M. Lu, S.-J. Park, B. T. Cunningham, and J. G. Eden, "Transparent Plastic Microplasma Flexible Light Sources," *IEEE Trans. Plasma Sci.,* vol. 4, p. 430, 2006

[4] M. Lu, S.-J. Park, B. T. Cunningham, and J. G. Eden, "Microcavity plasma devices and arrays fabricated by plastic-based replica molding," *J. Micro-electromech. Syst.,* vol. 16, no. 6, pp. 1397-1402, Dec. 2007

[5] B. T. Cunningham, P. Li, S. Schulz, B. Lin, C. Baird, J. Gerstenmaier, C. Genick, F. Wang, E. Fine, and L. Laing, "Label-free assays on the BIND system," *Journal of Bimolecular Screening,* vol. 9, pp. 481-490, 2004

[6] S. J. Park, K. S. Kim, and J. G. Eden, "Ultraviolet emission intensity, visible luminance, and electrical characteristics of small arrays of Al/Al_2O_3 microcavity plasma devices operating in Ar/N_2 or Ne at high-power loadings," *J. Appl. Phys.,* vol. 99, p. 026107, 2006

[7] —, "Nanoporous alumina as a dielectric for microcavity plasma devices: Multilayer Al/Al_2O_3 structures," *Appl. Phys. Lett.,* vol. 86, p. 221501, 2005

[8] S. –J. Park, C. J. Wagner, C. M. Herring, and J. G. Eden, "Flexible microdischarge arrays: Metal/polymer devices," *Appl. Phys. Lett.,* vol. 77, pp. 199-201, 2001

[9] R. Foest, M. Schmidt, and K. Becker, "Microplasmas, an emerging field of low-temperature plasma science and technology," *Int. J. Mass. Spectrum.,* vol. 248, pp. 87-102, 2006

[10] J. Zheng, J. Y. Kim, S. K. Lee, S.-J. Park, and J. G. Eden, "Molded Arrays of Microcavities and Channels in Polymer Structure: Ultraviolet Emitting Microplasma Sources for Biophotonics," *IEEE Trans. Plasma Sci.,* vol. 36, no. 4, pp. 1256-1257, Aug. 2008

[11] A. D. White, "New Hollow Cathode Glow Discharge," *Journal of Applied Physics,* vol. 30, pp. 711, 1959

[12] V. Puech, F. Collier, and P. Cottin, "Energy transfer between electronically excited argon and nitrogen: A kinetic model for the 3371 and the 3577 Å laser emissions," *J. Chem. Phys.* vol. 67, 2887, 1977

[13] S. K. Searles, and G. A. Hart, "Laser emission at 3577 and 3805 Å in electron-beam-pumped $Ar\text{-}N_2$ mixtures," *Appl. Phys. Lett.* vol. 25, pp. 79, 1974

[14] F. Abdelmalet, M. R. Ghezzar, M. Belhadj, A. Addou, and J.-L. Brisset, "Bleaching and Degradation of Textile Dyes by Nonthermal Plasma Process at Atomospheric Pressure," Ind. Eng. Chem. Res., vol. 45, pp. 23-29, 2006

[15] B. J. Ricconi, S.-J. Park, S. H. Sung, P. A. Tchertchian, and J. G. Eden, "OH(A $^2\Sigma^+$) and rare gas-deuteride (NeD, ArD) excimers generated in microcavity plasmas: ultraviolet emission spectra and formation kinetics," *Appl. Phys. Lett.,* vol. 90, no. 20, pp. 201504-1-3, May 2001

[16] C. Guillen and J. Herreo, "Comparison study of ITO thin films deposited by sputtering at room temperature onto polymer and glass substrates," *Thin Solid Films,* vol. 480, pp. 129-132, 2005

[17] A. Norris, "Silicones: ideal material solutions for the photovoltaic industry," *Photovoltaics International*, pp. 11-12, 2009

[18] A. V. Engel, *Ionized Gases.* Woodbury, NY: AIP Press, 1994

[19] J. D. Readle, K. E. Tobin, K. S. Kim, J. K. Yoon, J. Zheng, S. K. Lee, S.-J. Park, and J. G. Eden, "Flexible, Lightweight Arrays of Microcavity Plasma Devices: Control of Cavity Geometry in Thin Substrates," *IEEE Trans. Plasma Sci.,* vol. 37, no. 6, p. 1045, 2009